A valence bond description of the bromine halogen bond

Davide Franchini,[1] Alessandro Genoni, [3*] Federico Dapiaggi,[1] Stefano Pieraccini,[1,2*] and Maurizio Sironi[1,2*]

Correspondence to: Maurizio Sironi (E-mail: maurizio.sironi@unimi.it)

[1] Davide Franchini, Federico Dapiaggi, Stefano Pieraccini, and Maurizio Sironi
Dipartimento di Chimica and INSTM UdR, Università degli Studi di Milano
Via Golgi 19, 20133, Milano (Italy)
[2] Stefano Pieraccini, and Maurizio Sironi
CNR-ISTM (Istituto di Scienze e Tecnologie Molecolari del CNR) and INSTM UdR
Via Golgi 19, 20133, Milano (Italy)
[3] Alessandro Genoni
Université de Lorraine & CNRS, Laboratoire de Physique et Chimie Théoriques (LPCT), UMR CNRS 7019, 1 Boulevard Arago, F-57078 Metz, France.

ABSTRACT

A theoretical investigation on the nature of the halogen bond through a Valence-Bond approach has been carried out with two main goals: i) finding further confirmations of already existing explanations on the physical origins of the halogen bond and ii) possibly enriching the current models with new details. To achieve these goals we have exploited the spin-coupled method and we have performed computations on RBr···NH3 dimers characterized by a different electron withdrawing power of substituent –R to the bromine atom. The analysis of typical spin-coupled descriptors (e.g., shapes and overlaps of the spin-coupled orbitals, weights of the spin-coupled structures) in the different cases and in function of the distance between the monomers allowed us to draw qualitative conclusions about the formation and the strength of the halogen bonds. In particular, the investigation not only confirmed the validity of already existing models (i.e., σ-hole and lump-hole models) but also highlighted interesting new features, such as the fact that the depletion of electron density around the bromine atom does not extend only towards the acceptor of the halogen bond, but also in the opposite direction (towards the substituent of the halogen), thus forming a sort of σ-tunnel, rather than a simple σ-hole.

Introduction

Halogen bonding (XB) is an interesting non-covalent interaction[1,2] that establishes between a halogen atom X (covalently bonded to a substituent group R) and an acceptor group B characterized by a nucleophilic character, following the general scheme R-X···B. There are several factors that contribute to determine the strength of this peculiar bonding interaction. The most important ones are i) the electron withdrawing power of the substituent group R, ii) the polarizability of the halogen atom (I > Br > Cl >> F) and, finally, iii) the basicity of the acceptor group B.

Despite its peculiar nature, basically consisting in a halogen atom acting as electrophile, XB interaction has been only barely studied in the past and it has become a hot topic only quite recently. In fact, also as a consequence of more and more detailed investigations that allowed us to gain fundamental insights into the nature of the interaction, several research groups have already envisaged the possibility of exploiting halogen bonding for functional applications.

Among them we can mention applications in medicinal chemistry and, particularly, in the rational design of new drugs. In fact, experimental evidences have interestingly shown that halogen bonds are able to efficiently stabilize protein-ligand complexes[3-5]

and to compete with hydrogen bonds in stabilizing DNA junctions through brominated uracil-bases[6]. The importance of these observations is further enhanced by the fact that halogenated drugs are generally characterized by increased half-lives and better membrane permeability, which really makes halogen bond a fundamental key-interaction in modern rational drug design.

Moreover, since XB interactions have been shown very efficient in tuning material properties (e.g., optical or magnetic properties)[7,8] and in directing supramolecular assemblies[9-12], two important and related fields where halogen bond currently plays a crucial role are Materials Science and Crystal Engineering.[13,14]

As mentioned above, several efforts have been recently made i) to propose models with the aim of shedding further light on the nature of halogen bonding and ii) to develop new useful, theoretical/computational tools to correctly predict properties of halogen bond-based systems. For example, in the latter case, the increasing number of X-ray resolved protein structures with halogenated ligands led to the need of developing an efficient strategy to describe halogen bonds by means of classical force field methods.[15,16]

Concerning the different models for halogen bonding that have been proposed over the years, the one introduced by Politzer[17] could be probably considered as a milestone in this research area. In fact, it has been the first one to successfully and rationally describe the reason why commonly considered "negative atoms" as halogens interact with nucleophiles. According to this model, the establishment of a covalent R-X bond causes a depletion of electron density in the outward region of the halogen atom along the R-X bond direction (conventionally denoted as the z-axis throughout the paper), thus giving rise to a region of positive electrostatic potential (ESP), which is commonly called σ-hole, and a belt of negative ESP around this σ-hole to compensate it. This anisotropy of the ESP is the reason why halogens can interact with nucleophiles.

Moreover, the model explains i) the trend in the strength of halogen bonding, which is simply associated with the maximum value of the ESP in the σ-hole (for a given acceptor), and ii) the great directionality of the XB interaction, which is strictly related to the narrow localization of the σ-hole around the z-axis.

Another complementary model to the previous one is the lump-hole model[18] that relies on the physical interpretation of the Laplacian of the electron density, $\nabla^2\rho(r)$. Following Bader's Quantum Theory of Atoms in Molecules,[19] $\nabla^2\rho(r)$ can be used to distinguish between regions characterized by concentration ($\nabla^2\rho(r) < 0$) and depletion of electron density ($\nabla^2\rho(r) > 0$). Therefore, following this interpretation, in case of an XB interaction there will be an electron density depletion region ($\nabla^2\rho(r) > 0$), the hole, in proximity of the halogen atom and an electron density concentration region ($\nabla^2\rho(r) < 0$), the lump, localized on the acceptor. As the halogen atom approaches towards the acceptor, the hole will interact with the lump in a key-lock mechanism, thus leading to the establishment of the interaction.

All the previous models have been fully confirmed by accurate experimental charge density studies[20] and by several theoretical calculations.[21] Nevertheless, to the best of our knowledge, the computations have been almost exclusively performed in the framework of Molecular Orbital (MO)-based techniques. Valence Bond (VB) strategies have been rarely exploited in this context,[22] although, due to their intrinsic "chemical nature", the latter could provide significant insights into the features of the halogen bonding interaction. In fact, in all VB techniques, molecular electronic structure is described in terms of orbitals that are mainly localized on atoms and that significantly overlap when bonding interactions occur, thus preserving the traditional chemical picture of bond as schematically depicted through the well-known Lewis molecular structures. On the contrary, this traditional description is completely lost in all those computational strategies based on MOs since,

in general, the obtained orbitals are completely delocalized on the whole systems under exam. Several efforts have been made to recover traditional chemical concepts (e.g., bond- and lone-pairs) also from MO-based calculations. For example, it is worth mentioning the a posteriori methods,[23-27] which allow the determination of Localized Molecular Orbitals (LMOs) as unitary transformation of canonical Hartree-Fock MOs, or the a priori techniques,[28-46] which exploit user-defined and chemically meaningful localization schemes to compute MOs that are extremely localized on small molecular fragments (atoms, bonds or functional groups) and that are easily transferable from a molecule to another.[47-53] Attempts of exploiting localized MOs in a Valence Bond way were also proposed[54-57] but, notwithstanding all these efforts, pure VB approaches remain the closest theoretical methods to traditional chemical concepts, although they are more computationally expensive than those based on MOs.

In this paper, also following the example of McAllister et al., who tried to rationalize and get further insights into the nature of halogen-bonds between halomethanes and rare gases in terms of localized molecular orbitals,[58] we present one of the first Valence Bond-based investigations on the nature of halogen bond. Here it is worth noting that our study mainly aimed at using fully VB concepts both to qualitatively confirm the validity of well-established models for the halogen bonding and to seek additional insights into the physical origin of this interaction.

To accomplish this task we have decided to resort to a particular VB strategy: the spin-coupled (SC) method,[59-61] which will be briefly described in the Theory section and which has been also recently combined with the X-ray constrained wave function approach[62,63] of quantum crystallography[64,65], giving rise to the new XC-SC strategy[66] that can be potentially used for the extraction of chemically meaningful information (e.g., resonance structure weights, electron correlation effects[67], etc.) from high-resolution X-ray diffraction data.

To investigate the nature of the XB interaction, we have performed Spin-Coupled calculations on different RBr⋯NH3 dimers (R = −H, HCC−, −CN). In this way it was possible to draw some conclusions about the formation and the strength of the halogen bond in the different cases in terms of spin-coupled orbitals, their overlaps and weights of the spin-coupled structures. Finally, the obtained results have been discussed in function of the Politzer and lump-hole models mentioned above, showing that also VB calculations fully confirm them.

The paper is organized as follows: after a brief overview of the spin-coupled technique, we will dedicate a section dedicated to describe the strategies used to investigate the formation and strength of the halogen bond in the RBr⋯NH3 dimers. Afterwards, we will present and discuss the obtained results and, finally we will draw our final conclusions trying to find a connection between the outcomes of our calculations and commonly accepted models for interpreting and rationalizing the halogen bonding interaction.

Theory

In the spin-coupled method, the wave function for a system of N electrons is written by using non-orthogonal singly occupied orbitals that can interact by overlapping between themselves. Due to the non-orthogonality and the single occupancy of the spin-coupled orbitals there is, almost always, more than one way for coupling the individual spin of the N electrons to obtain the total spin of the system. These different coupling possibilities correspond to different spin-coupled structures. In particular, it is possible to show that, in case of a system of N electrons with total spin S, for each value M[68] of the projection of S, we can write f_S^N linearly independent spin-coupled structures (and spin-eigenfunctions), where f_S^N is defined as:

$$f_S^N = \frac{(2S+1)N!}{\left(\frac{1}{2}N + S + 1\right)!\left(\frac{1}{2}N - S\right)!} \quad (1)$$

Consequently, by associating each possible spin-coupled structure with a particular N-electron function $\psi_{S,M;k}^N$, the global SC wave function for a system of N electrons in a spin-state (S, M) can be expressed as follows:

$$\psi_{SC}^{S,M} = \sum_{k=1}^{f_S^N} c_{sk}\, \psi_{S,M;k}^N$$

$$= \sum_{k=1}^{f_S^N} c_{Sk} \mathcal{A}\left(\Phi\, \Theta_{S,M;k}^N\right) \quad (2)$$

where $\mathcal{A}$ is the usual antisymmetrizing operator, $\Theta_{S,M;k}^N$ is the k-th spin-eigenfunction for the N-electron system in the spin-state (S, M), Φ is the product of N spatial functions $\{\phi_i\}_{i=1}^N$ (namely, the spin-coupled orbitals)

$$\Phi\left(\mathbf{r}_1, \mathbf{r}_2, \dots \mathbf{r}_N\right)$$
$$= \phi_1(\mathbf{r}_1)\, \phi_2(\mathbf{r}_2) \dots \phi_N(\mathbf{r}_N) \quad (3),$$

and $c_{S,k}$ are the spin-coupling coefficients that are used to weight the importance of each spin-coupled structure in the wave function $\psi_{SC}^{S,M}$, also through the determination of the Chirgwin-Coulson coefficients[69] defined like this:

$$w_{S,k} = \left|c_{S,k}\right|^2 + \sum_{j \neq k}^{f_S^N} c_{S,k}\, c_{S,j}\, S_{kj} \quad (4)$$

with S_{kj} as the overlap integral between the spin-coupled structures $\psi_{S,M;k}^N$ and $\psi_{S,M;j}^N$

It is worth noting that, to reduce the computational cost associated with the spin-coupled calculations, it is also usually advisable to subdivide the N electrons of the systems into two groups: a subset of $2N_1$ core electrons and a subset of N_v valence electrons. The former can be described by frozen doubly occupied Molecular Orbitals previously obtained by means of a proper Hartree-Fock computation on the system under exam. Since Molecular Orbitals are generally delocalized on the whole molecule, they are usually localized to better decide which of them to freeze. The valence electrons are really described at spin-coupled level. Therefore, in these cases, the spin-coupled wave function assumes this form:

$$\psi_{SC}^{S,M} = \sum_{k=1}^{f_S^{N_v}} c_{sk}\, \psi_{S,M;k}^N$$

$$= \sum_{k=1}^{f_S^{N_v}} c_{Sk}\, \mathcal{A}\left(\phi_1^c\, \overline{\phi}_1^c \dots \phi_{N_1}^c\, \overline{\phi}_{N_1}^c\, \Phi_v\, \Theta_{S,M;k}^{N_v}\right) \quad (5)$$

where c_{Sk} and $\mathcal{A}$ have an analogous meaning to the one seen for equation (2), ϕ_i^c is a frozen "core spin-orbital" with spatial part ϕ_i^c and spin part α, $\overline{\phi}_i^c$ is a frozen "core spin-orbital" with spatial part ϕ_i^c and spin part β. As already mentioned above, the spatial parts $\{\phi_i^c\}$ can be canonical Molecular Orbitals or localized Molecular Orbitals. Furthermore, $\Theta_{S,M;k}^{N_v}$ is the k-th spin-eigenfunction for the N_v valence electrons in the spin-state (S, M), and Φ_v is the product of the N_v "valence spin-coupled orbitals", namely:

$$\Phi_v\left(\mathbf{r}_1, \mathbf{r}_2, \dots \mathbf{r}_{N_v}\right)$$
$$= \phi_1^v(\mathbf{r}_1)\, \phi_2^v(\mathbf{r}_2) \dots \phi_{N_v}^v\left(\mathbf{r}_{N_v}\right) \quad (6)$$

Due to the doubly occupancy of the core orbitals, the active SC orbitals can be assumed orthogonal to the core orbitals without losing generality. In order to easily accomplish this, the active SC orbitals are expanded over the set of MOs $\left\{\phi_\mu(r)\right\}_{\mu=N_1+1}^M$ consisting of the remaining (localized or canonical) occupied Hartree-Fock Molecular Orbitals and of all the virtual Hartree-Fock Molecular Orbitals, i.e.:

$$\phi_i^v(\mathbf{r}) \sum_{\mu=N_1+1}^M C_{\mu i}\, \phi_\mu(r) \quad (7)$$

where M is the dimension of the adopted basis-

set (namely, the number of atomic orbitals initially used to perform the preliminary Hartree-Fock calculation). In this way the active SC orbitals are described using the full basis-set with the only constraint to be orthogonal to the frozen core orbitals.

The coefficients $\{C_{\mu i}\}$ of the spin-coupled orbitals expansions are thus obtained together with the spin-coupling coefficients $\{c_{S,k}\}$ (see equations (2) and (5)) by variationally minimizing the following energy functional:

$$W[\{C_{\mu i}\},\{c_{Sk}\}] = \frac{\langle \psi_{SC}^{S,M}|\hat{H}|\psi_{SC}^{S,M}\rangle}{\langle \psi_{SC}^{S,M}|\psi_{SC}^{S,M}\rangle} \quad (8)$$

with $\hat{H}$ as the traditional non-relativistic Hamiltonian operator for a system of N electrons.

Methods

To investigate formation and strength of the halogen bond in RBr···NH3 dimers, we have considered three different –R substituents for the bromine atom: –H, HCC– (acetylene group) and –CN (cyano group), clearly characterized by an increasing electron withdrawing power and, consequently, responsible for stronger halogen bonds.

To monitor the formation of a halogen bonding interaction in the RBr···NH3 dimers, we carried out spin-coupled calculations at different geometries previously obtained through relaxed geometry scans at Restricted Hartree-Fock (RHF) / 6-31G(d,p)[70] level in which we varied the Br ···N distance (from 2.39 Å to 7.79 Å for (CN)Br···NH3, from 2.51 Å to 5.01 Å for HCCBr···NH3 and from 2.58 Å to 5.68 Å for HBr···NH3) and in which we constrained the R-Br···N angle equal to 180°. Finally, for all the three dimers we have also considered the corresponding asymptotic structures, basically corresponding to the two isolated monomers RBr and NH3 at very large distance (R-Br··· N angle always constrained to 180°).

The obtained geometries for the RBr···NH3 dimers have been afterwards exploited to

perform single point spin-coupled calculations with only 10 active electrons (corresponding to valence electrons in equations (5) and (6)). The remaining electrons (core electrons in equations (5) and (6)) were described through frozen doubly occupied Localized Molecular Orbitals) resulting from the application of the Pipek-Mezey localization technique to occupied Molecular Orbitals previously obtained through RHF calculations. These orbitals correspond to the frozen "core SC orbitals" in equation (5).

For this reason, in all our SC computations, only ten spin-coupled orbitals were directly optimized. They describe the three-bromine lone-pairs, the nitrogen lone-pair and the R-Br bond electron-pair. As briefly mentioned in the Theory section, the "valence SC orbitals" have been obtained by fully expanding them, without any symmetry constraint, in the set of orbitals consisting of the remaining occupied Pipek-Mezey LMOs (i.e., the non-frozen ones) and of the virtual (and completely delocalized) RHF MOs of the system under exam. So, for each SC orbital, the guess was a linear combination of the unfrozen occupied Pipek-Mezey LMOs and of the virtual RHF MOs. As mentioned above, it is worth stressing that, unlike the occupied Pipek-Mezey LMOs, the virtual molecular orbitals are completely delocalized on the investigated systems and, therefore, this allowed us to set up an educated and, at the same time, quite general guess without biasing the following spin-coupled calculations.

The 10 singly occupied spin-coupled orbitals (see Figures S1 and S2 for two- and three-dimensional graphical representations of the SC orbitals in the (CN)Br···NH3 case at asymptotic distance) resulting from our computations were afterwards classified, by observing their components expressed in atomic orbitals basis, and labeled in this way (always assuming the R-Br bond axis as the z-axis):

- ϕ_1: sp$_z$-like hybrid orbital mainly localized on the bromine atom and deformed toward the substituent R. It is worth noting that this orbital is

characterized by a hole that can be associated with the σ-hole of the Politzer model.

- ϕ_2: sp_z-like hybrid orbital mainly localized on the carbon atom ((CN)Br and HCCBr) or the hydrogen atom (HBr) and deformed toward the bromine atom.

- ϕ_3, ϕ_4: orbitals resembling sp_z hybrid lone-pair orbitals localized on the bromine atom, both of them characterized by a non-negligible σ component. ϕ_3 is more contracted along the z-axis, while ϕ_4 is more spread towards the two directions perpendicular to the z-axis.

- ϕ_5, ϕ_6: orbitals resembling p_y lone-pair orbitals localized on the bromine atom. Both of them are characterized by a weak, but non-negligible, σ component and by a small overlap with orbitals ϕ_3 and ϕ_4.

- ϕ_7, ϕ_8: orbitals resembling p_x lone-pair orbitals localized on the bromine atom. Both of them are characterized by a weak, but non-negligible, σ component and by a small overlap with orbitals ϕ_3 and ϕ_4. They are symmetry related to orbitals ϕ_5 and ϕ_6.

- ϕ_9, ϕ_{10}: orbitals describing the p_z lone-pair localized on the nitrogen atom. ϕ_9 is more spread towards the direction of the bromine atom than orbital ϕ_{10}.

Afterwards, they were analyzed by monitoring some of their overlaps and some of their square moduli differences, both in function of the Br···N distance and in function of the substituent group R. As we will explain in the Results section, this allowed us to detect partial delocalizations clearly associable with the presence of a halogen-bond interaction.

Moreover, it is worth noting that, according to equation (1), the 10 active electrons (and consequently the 10 associated SC orbitals mentioned above) in a singlet state can be spin-coupled in 42 different ways, which correspond to 42 different spin-coupled structures contributing to the global SC wave function (see Equation (5)). In order to have a direct connection with the traditional Lewis chemical structures, the Rumer spin eigenfunctions basis was adopted.[71,72] The weights of all the structures have been also carefully monitored in function of the Br···N distance and in function of the substituent group R to study the formation and the strength of the halogen-bond in the investigated systems.

To obtain the dimers geometries the Gaussian09[73] software has been adopted, while, for the SC calculations, a code developed in our research group has been used.[74]

Results

As mentioned in the previous section, different descriptors were considered to study the formation and the strength of the halogen bond in the investigated RBr···NH3 dimers: overlap between the SC orbitals, shape of the SC orbitals and weight of the spin-coupled structures.

At first, we mainly focused on the analysis of the overlap integrals between the 10 optimized SC orbitals already described in the previous section. In particular, since orbitals ϕ_9 and ϕ_{10} are mainly localized on the nitrogen atom, we decided to monitor their overlaps with the other eight SC orbitals (mainly localized on Br) in function of the distance, with the aim of possibly correlating their expansions towards the bromine atom with the formation of the halogen bond. From our computations, we have immediately observed that, as expected, for all the different Br···N distances, the largest overlaps of ϕ_9 and ϕ_{10} (the orbitals describing the nitrogen lone-pair) were with z-symmetry orbitals (ϕ_1, ϕ_2, ϕ_3 and ϕ_4), while the overlaps with the other SC orbitals were almost negligible. In particular, the greatest overlaps of ϕ_9 and ϕ_{10} are with orbital ϕ_1, which, from a

Valence Bond point of view, could be the main responsible for the halogen bond interaction. In fact, as mentioned above and as it can be clearly seen in Figure S1, this orbital is characterized by a hole that can be easily associated with the the σ-hole on the Br atom. In Figure 1, we have also graphically depicted how the overlaps of ϕ_9 (Figure 1A) and ϕ_{10} (Figure 1B) with ϕ_1, ϕ_2, ϕ_3 and ϕ_4 vary in function of the Br⋯N distance for the (CN)Br⋯NH3 dimer. It is easy to observe that, both for ϕ_9 and for ϕ_{10}, the overlaps increase as the two monomers approach, thus revealing the possible presence of a halogen bond interaction at shorter distances. Analogous trends have been also noted for the HCCBr⋯NH3 and HBr⋯NH3 dimers (see Figures

S3 and S4 in the Supplementary Material), although it is immediately evident that the overlaps magnitudes decrease when substituents HCC– and –H are taken into account. This can be also evinced from Table 1, where we have reported the overlaps at the equilibrium distances for the three investigated systems, which confirms that the strength of the halogen bond decreases as the electron-withdrawing character of the R substituent reduces.
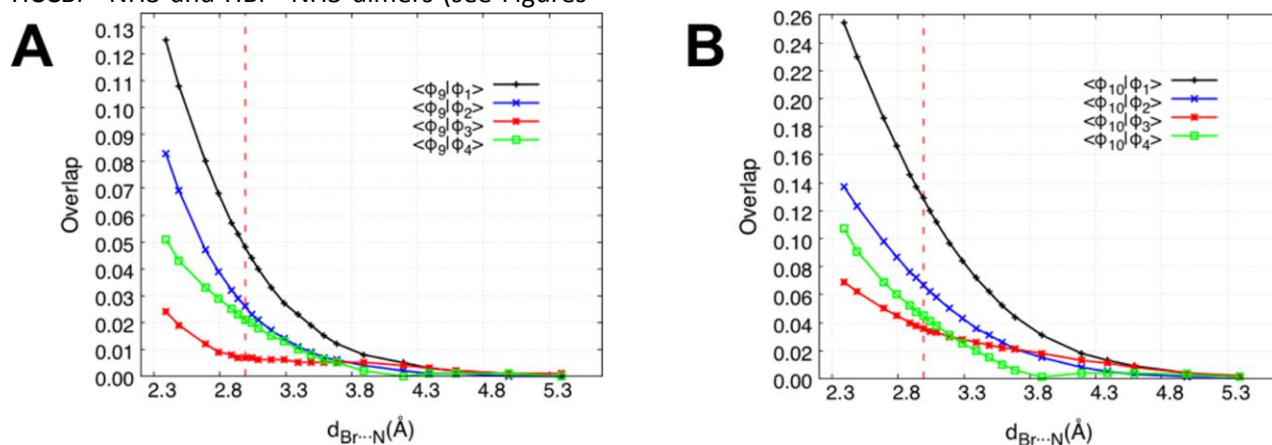

Figure 1. Overlaps of the spin-coupled orbitals ϕ_9 and ϕ_{10} with the spin-coupled orbitals ϕ_1, ϕ_2, ϕ_3 and ϕ_4 in function of the Br⋯N distance for the (CN)Br⋯NH3 dimer. The vertical red dotted lines indicate the Br⋯N equilibrium distance.

Table 1. Absolute values of the overlaps of the spin-coupled orbitals ϕ_9 and ϕ_{10} with the spin-coupled orbitals ϕ_1, ϕ_2, ϕ_3 and ϕ_4 at the equilibrium distances for the dimers (CN)Br···NH3, HCCBr··· NH3 and HBr··· NH3

	(CN)Br···NH$_3$		HCCBr··· NH$_3$		HBr··· NH$_3$	
	ϕ_9	ϕ_{10}	ϕ_9	ϕ_{10}	ϕ_9	ϕ_{10}
ϕ_1	0.048	0.129	0.037	0.103	0.028	0.085
ϕ_2	0.026	0.067	0.019	0.054	0.015	0.047
ϕ_3	0.021	0.045	0.008	0.035	0.010	0.023
ϕ_4	0.007	0.036	0.015	0.029	0.008	0.028

A second descriptor to reveal the presence of an XB interaction in the examined systems was the shape of the obtained orbitals. At first, we have considered orbitals ϕ_9 and ϕ_{10}, which are mainly localized on the nitrogen atom. For each of them, we have evaluated and plotted the difference between their squared moduli at the equilibrium and asymptotic distances (i.e., $\left|\phi_9^{eq}\right|^2 - |\phi_9^\infty|^2$ and $\left|\phi_{10}^{eq}\right|^2 - |\phi_{10}^\infty|^2$). The obtained differences for the (CN)Br···NH3 dimer are depicted in Figures 2A and 2B, where we can easily observe that both orbitals ϕ_9 and ϕ_{10} are more localized on the nitrogen atom at the asymptotic distance, while they clearly shift towards the bromine atom at the equilibrium distance. Moreover, the effect is much more evident for orbital ϕ_{10} than for orbital ϕ_9. Also these observations can be considered as another clear evidence of the formation of a halogen bond interaction RX···B at the equilibrium distance and can be rationalized though a "pictorial" chemical representation in which one electron of the lone-pair localized on acceptor atom B "moves" towards electrophilic region X, while the other electron of the pair remains on the nucleophilic site. Furthermore, it is quite interesting and unexpected that, during the formation of the halogen bond, the spin-coupled orbital (ϕ_{10}) describing the

electron donated by acceptor B (in this case the nitrogen atom), also delocalizes over the region of the C-Br bond and not only outward this bond (see Figures 2B, 2D and 2F). This can be interpreted (from a valence-bond point of view) as if the σ-hole, which is usually observed along the z-axis, in the region outward the halogen atom, existed also behind the halogen in the direction of the substituent group R. The calculation of the RHF/6-31G(d,p) electrostatic potential in the xz plane indeed shows (see Figure 3) that the depletion of electron density along the z-axis around the halogen atom is not only localized outward the halogen atom, but it can be also seen as an extended positive region of electrostatic potential along the R-Br bond. Therefore, the σ-hole could be actually seen as a "σ-tunnel" in terms of spin-coupled orbitals. This positive region of electrostatic potential attracts negative electron density from acceptor B and this is probably the reason why, in all our spin-coupled calculations performed at the equilibrium distances, the largest overlaps for the "shifted" (see Figure 2) orbitals ϕ_9 and ϕ_{10} have been observed with orbital ϕ_1 (see Figure 1), namely the orbital characterized by a hole on the Br atom ascribable to the σ-hole of the Politzer model .

For the sake of completeness, in Figure 2 we have also reported the differences between the

squared moduli of orbitals ϕ_9 and ϕ_{10} at the equilibrium and asymptotic distances for the dimers HCCBr⋯NH3 (Figures 2C and 2D) and HBr⋯NH3 (Figures 2E and 2F). Although of lower extent, the trends are analogous to those observed for (CN)Br⋯NH3, further indicating that the strength of the XB interaction reduces when a less electron-withdrawing group is bonded to the halogen atom.
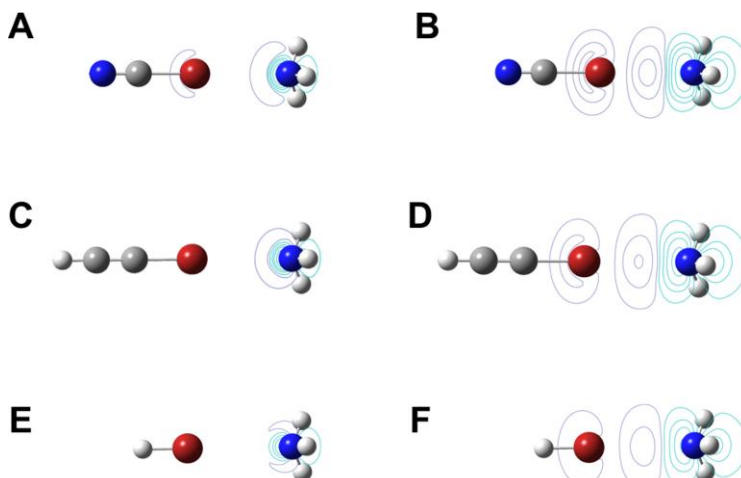

Figure 2. Differences between the squared moduli of the spin-coupled orbitals ϕ_9 (A, C and E) and ϕ_{10} (B, D and F) at the equilibrium and asymptotic distances for the dimers (CN)Br⋯NH3 (A, B), HCCBr⋯NH3 (C, D) and HBr⋯NH3 (E, F). Positive and Negative contour levels are depicted in purple and light blue, respectively. The absolute values (in au) of the positive and negative contours increase in steps of 2×10^n, 4×10^n and 8×10^n, with n ranging from -3 to 0 and increasing by 1 at every step. The contours levels of 5×10^{-4} au and 1×10^{-4} au have been added for the sake of completeness, both for the negative and positive contours.

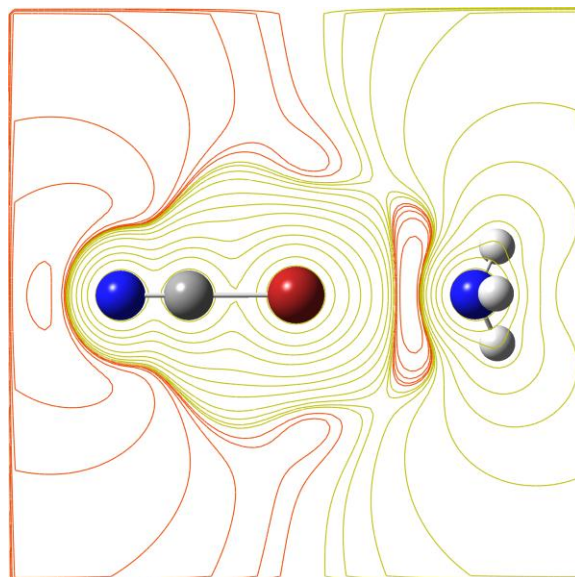**Figure 3.** Contour levels of the Electrostatic Potential in the xz plane for the (CN)Br⋯ NH3 dimer. Positive and Negative contour levels are depicted in yellow and orange, respectively. The absolute values (in au) of the positive and negative contours increase in steps of 2×10^n, 4×10^n and 8×10^n, with n ranging from -3 to 0 and increasing by 1 at every step. The contours levels of 5×10^{-4} au and 1×10^{-4} au have been added for the sake of completeness, both for the negative and positive contours.

Finally, we have considered the Br-centered and z-symmetry orbitals ϕ_1, ϕ_3 and ϕ_4. Also in this case, we have evaluated and plotted the differences between their squared moduli at the equilibrium and asymptotic geometries. The results obtained for (CN)Br⋯NH3 (Figure 4), HCCBr⋯NH3 (Figue 5) and HBr⋯NH3 (Figure 6) are completely analogous and show that, at the equilibrium distance, the three examined spin-coupled orbitals shift/delocalize towards the substituent group R. This leaves a depletion of charge around the bromine atom that can be easily associated with the σ-hole of the Politzer model. Hence, this is another evidence of the existence of halogen bonds when we are at the equilibrium geometry. However, the entity of the orbitals delocalizations does not change significantly among the different dimers and, therefore, in this case, from Figures 4, 5 and 6 we cannot infer on the strength of the different halogen bonds.
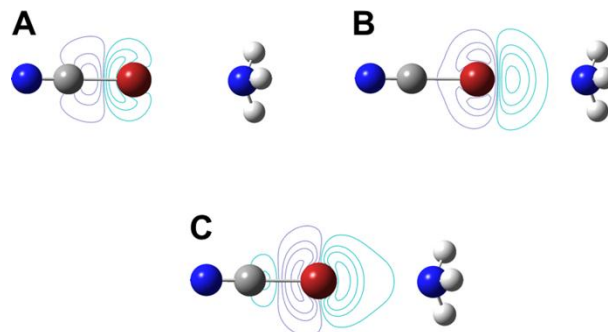

Figure 4. Differences between the squared moduli of the spin-coupled orbitals ϕ_1 (A), ϕ_3 (B) and ϕ_4 (C) at the equilibrium and asymptotic distances for the (CN)Br⋯NH3 dimer. Positive and Negative contour levels are depicted in purple and light blue, respectively. The absolute values (in au) of the positive and negative contours increase in steps of 2×10^n, 4×10^n and 8×10^n, with n ranging from -3 to 0 and increasing by 1 at every step. The contours levels of 5×10^{-4} au and 1×10^{-4} au have been added for the sake of completeness, both for the negative and positive contours.
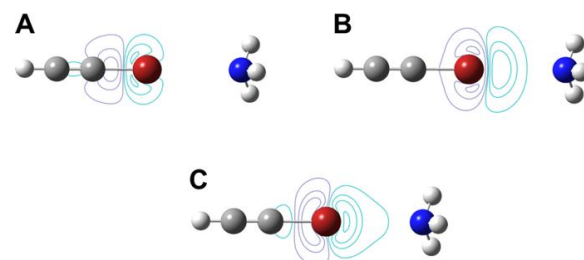

Figure 5. Differences between the squared moduli of the spin-coupled orbitals ϕ_1 (A), ϕ_3 (B) and ϕ_4 (C) at the equilibrium and asymptotic distances for the HCCBr⋯NH3 dimer. Positive and Negative contour levels are depicted in purple and light blue, respectively. The absolute values (in au) of the positive and negative contours increase in steps of 2×10^n, 4×10^n and 8×10^n, with n ranging from -3 to 0 and increasing by 1 at every step. The contours levels of 5×10^{-4} au and 1×10^{-4} au have been added for the sake of completeness, both for the negative and positive contours

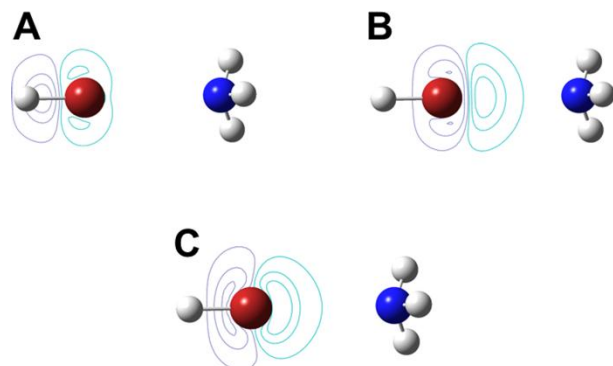**A**

B

C

Figure 6. Differences between the squared moduli of the spin-coupled orbitals ϕ_1 (A), ϕ_3 (B) and ϕ_4 (C) at the equilibrium and asymptotic distances for the HBr$\cdots$NH3 dimer. Positive and Negative contour levels are depicted in purple and light blue, respectively. The absolute values (in au) of the positive and negative contours increase in steps of 2×10^n, 4×10^n and 8×10^n, with n ranging from -3 to 0 and increasing by 1 at every step. The contours levels of 5×10^{-4} au and 1×10^{-4} au au have been added for the sake of completeness, both for the negative and positive contours.

As mentioned above, to complete our Valence Bond investigation of the halogen bond interaction, we have also decided to consider the weights of the different SC structures that contribute to the global spin-coupled wave functions. In particular, we have decided to monitor how the absolute values of the Chirgwin-Coulson coefficients associated with the different SC structures vary in function of the Br$\cdots$N distance in the different cases.

We have already pointed out that the 10 active electrons of our singlet-state systems can be potentially spin-coupled in 42 different ways corresponding to 42 spin-coupled structures in wave function (5). However, in the range of the Br$\cdots$N distances examined with our calculations, we have observed that only 5 structures are characterized by Chirgwin-Coulson coefficients significantly different from zero. Therefore, we considered them as the predominant SC structures for our systems and they were the only ones for which we have monitored the variation of the weight in function of the Br$\cdots$N distance. They are: i) the perfect pairing structure, namely the structure corresponding to spin-coupling $\phi_1 - \phi_2$ $\phi_3 - \phi_4$ $\phi_5 - \phi_6$ $\phi_7 - \phi_8$ $\phi_9 - \phi_{10}$ (from now on

indicated as structure 1); ii) structure 2, corresponding to spin-coupling $\phi_1 - \phi_4$ $\phi_2 - \phi_3$ $\phi_5 - \phi_6$ $\phi_7 - \phi_8$ $\phi_9 - \phi_{10}$; iii) structure 3, corresponding to spin-coupling $\phi_1 - \phi_9$ $\phi_2 - \phi_{10}$ $\phi_3 - \phi_4$ $\phi_5 - \phi_6$ $\phi_7 - \phi_8$; iv) structure 4, corresponding to spin-coupling $\phi_1 - \phi_4$ $\phi_2 - \phi_{10}$ $\phi_3 - \phi_9$ $\phi_5 - \phi_6$ $\phi_7 - \phi_8$; v) structure 5, corresponding to spin-coupling $\phi_1 - \phi_2$ $\phi_3 - \phi_9$ $\phi_4 - \phi_{10}$ $\phi_5 - \phi_6$ $\phi_7 - \phi_8$).

The first two structures correspond to the predominant ones at the asymptotic distances (i.e., for the isolated monomers), while structures 3, 4 and 5 are actually the ones that, from a traditional chemical point of view, can be easily associated with the formation of the halogen bonding interaction. In fact, each of them involves the pairing of a SC orbital localized on the nitrogen atom with a z-symmetry SC orbital localized on the bromine atom.

Although quite small, for all the investigated dimers, the Chirgwin-Coulson coefficients of structures 3-5 consistently increase as the two monomers approach and become significantly different from zero around the equilibrium distance (see Figure 7 for the (CN)Br$\cdots$NH3 dimer and Figures S5 and S6 in the Supplementary Material for the HCCBr$\cdots$NH3 and the HBr$\cdots$NH3 dimers, respectively). Therefore, considering the "chemical meaning" of structures 3-5 discussed above, we believe that this is a further indication of the existence of a halogen bond for the different systems at their equilibrium geometries. Furthermore, also in this case, we have clear evidences that the strength of the XB interaction increases with the electron-withdrawing power of the substituent group R. In fact, if we consider the weights of structures 3-5 at the Br$\cdots$N equilibrium distances (see Table 2), we can easily note that the largest and lowest values are observed for R=−CN and R=−H, respectively, which confirms the predicted trend according to the σ-hole model proposed by Politzer.
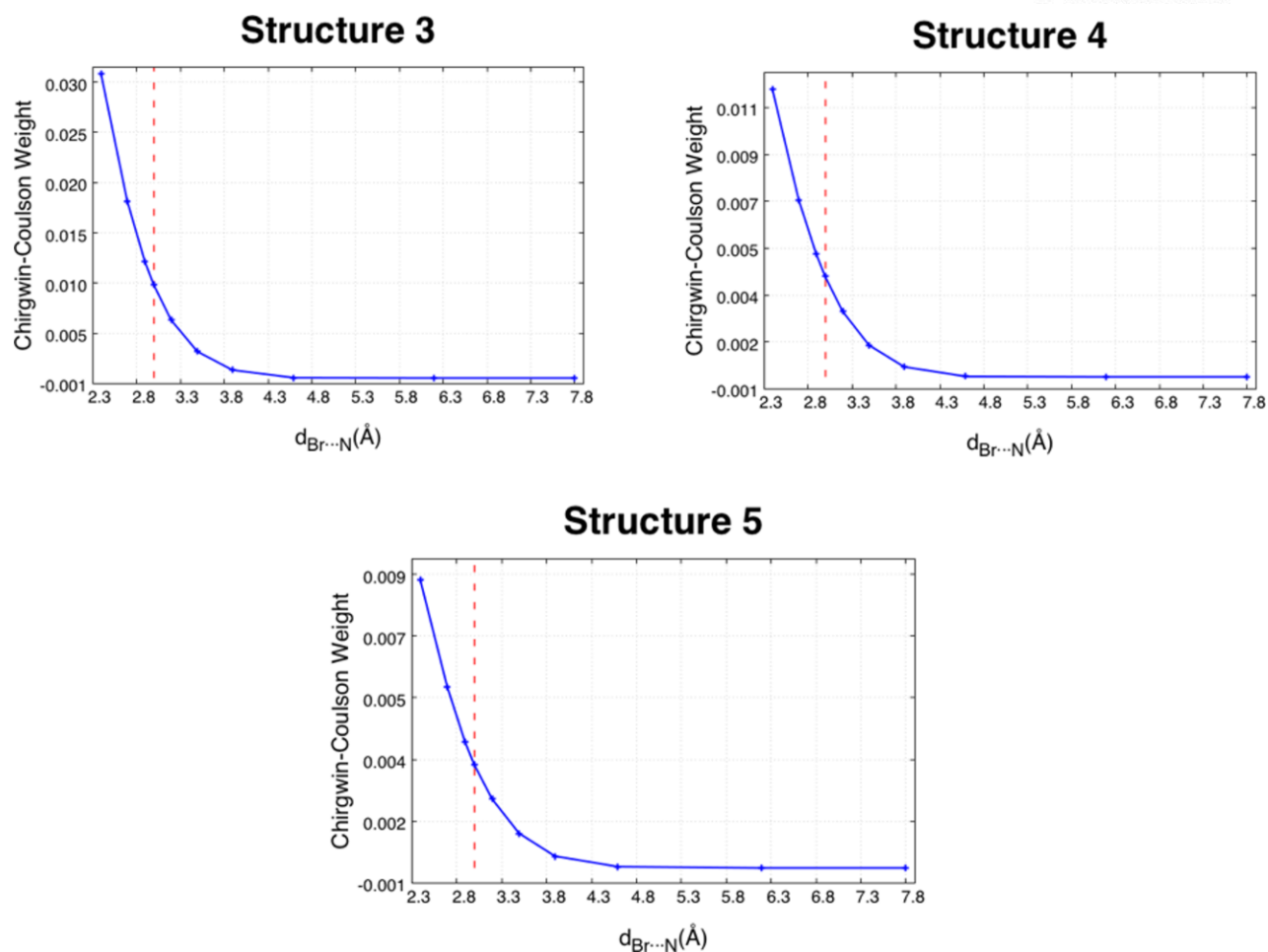
Structure 3

Structure 4

Structure 5

Figure 7. Absolute values of the Chirgwin-Coulson coefficients associated with structures 3, 4 and 5 of the (CN)Br···NH3 dimer in function of the Br···N distance. The vertical red dotted lines indicate the Br···N equilibrium distance.

Table 2. Absolute values of the Chirgwin-Coulson weights for spin-coupled structures 3, 4 and 5 of dimers (CN)Br···NH3, HCCBr··· NH3 and HBr··· NH3 at their Br···N equilibrium distances.

	(CN)Br···NH3	HCCBr···NH3	HBr··· NH3
Structure 3	9.35×10^{-3}	6.82×10^{-3}	4.93×10^{-3}
Structure 4	4.30×10^{-3}	3.31×10^{-3}	2.42×10^{-3}
Structure 5	3.34×10^{-3}	2.04×10^{-3}	7.9×10^{-4}

Conclusions

In this paper we have performed a Valence-Bond study of the halogen bond interaction exploiting the spin-coupled method and using the dimers (CN)Br···NH3, HCCBr···NH3 and HBr···NH3 as case studies. In particular, to investigate the nature and the strengths of the

Br···N interaction in the different systems, we have considered three different descriptors associated with the spin-coupled technique: the overlap between the spin-coupled orbitals, the shapes of these orbitals and the Chirgwin-Coulson weights of the spin-coupled structures. All these descriptors have not only shown that a Br···N interaction actually exists when the RBr

and NH3 monomers approach, but they were also able to confirm the expected trend for the strength of the interaction, as predicted by the Politzer and the lump-hole models for halogen bond.

Analyzing the overlaps and the shapes of the spin-coupled orbitals, we were also able to qualitatively confirm that, in presence of a halogen bonding interaction, a depletion of electron density occurs around the halogen atom (bromine in our case) with a consequent shift/delocalization of the electron density from the acceptor (nitrogen in our case) to the halogen. In other words, our spin-coupled calculations confirmed the mechanism of interaction described by the Politzer and lump-hole models (e.g. σ-hole and depletion of electron density around the halogen atom).

Moreover, analyzing our results we have also interestingly observed that, as a result of the halogen bond formation, the spin-coupled orbital describing one of the electrons of the donor's lone pair is localized on the halogen atom in the direction pointing towards the substituent group R of the halogen so that the σ-hole becomes a σ-tunnel for the spin-coupled orbitals. This agrees with simple calculations of electrostatic potentials that we have performed on the systems under exam.

Finally, it is worth pointing out again that the paper has reported only a qualitative investigation on the physical origin of the halogen bond in terms of traditional VB concepts/descriptors. However, given the success of the present study in confirming the validity of well-established models for the XB interaction, we expect that this can be the starting point for future and more quantitative investigations on halogen bonding through other Valence Bond techniques able to capture dynamic correlation effects, which are crucial to correctly take into account dispersion effects.

Acknowledgments

(Additional Supporting Information may be found in the online version of this article)

References and Notes

1. P. Metrangolo, G. Resnati, *Science* **2008**, *321*, 918.
2. P. Metrangolo, G. Resnati, Halogen Bonding: Fundamentals and applications; Springer: berlin, **2008**.
3. G. Cavallo, P. Metangolo, R. Milani, T. Pilati, A. Priimagi, G. Resnati, G. Terraneo, *Chem. Rev.* **2016**, *116*, 2478-2601.
4. Y. Lu, Y. Wang, W. Zhu, *Phys. Chem. Chem. Phys.* **2010**, *12*, 4543-4551.
5. P. Auffinger, F. A. Hays, E. Westhof, P. S. Ho, *PNAS* **2004**, *101* (48), 16789-16794.
6. A. R. Voth, F. A. Hays, P. S. Ho, PNAS **2007**, *104* (15), 6188-6193.
7. E. Cariati, A. Forni, S. Biella, P. Metrangolo, F. Meyer, G. Resnati, S. Righetto, E. Tordin, R. Ugo, *Chem. Commun.* **2007**, *0*, 2590-2592.
8. E. Cariati, G. Cavallo, A. Forni, G. Leem, P. Metrangolo, F. Meyer, T. Pilati, G. Resnati, S. Righetto, G. Terraneo, E. Tordin, Cryst. Growth Des. **2011**, 11 (12), 5642-5648.
9. P. K. Thallapally, G. R. Desiraju, M. Bagieu-Beucher, R. Masse, C. Bourgogne, J. Nicoud, *Chem. Commun.* **2002**, 1052–1053.
10. T. M. Beale, M. G. Chudzinski, M. G. Sarwar, M. S. Taylor, *Chem. Soc. Rev.* **2013**, *42* (4), 1667–1680.

11. A. Mele, P. Metrangolo, H. Neukirch, T. Pilati, G. Resnati, *J. Am. Chem. Soc.* **2005**, *127* (43), 14972–14973.

12. D. Mango, G. Barbato, S. Piccirilli, M. B. Panico, M. Feligioni, C. Schepisi, M. Graziani, V. Porrini, M. Benarese, A. Lanzillotta, M. Pizzi, S. Pieraccini, M. Sironi, F. Blandini, F. Nicoletti, N. B. Mercuri, B. P. Imbimbo, R. Nisticò, *Pharmacol. Res.* **2014**, *81*, 83-90.

13. A. Priimagi, G. Cavallo, P. Metrangolo, G. Resnati, *Acc. Chem. Res.* **2013**, *46 (11)*, 2686-2965.

14. P. Metrangolo, G. Resnati, *Chem. Europ. J.* **2001**, *7* (12), 2511-2519.

15. S. Rendine, S. Pieraccini, A. Forni, M. Sironi, *Phys. Chem. Chem.* Phys. **2011**, *13 (43),* 19508-19516.

16. M. A. A. Ibrahim, *J. Comput. Chem.* **2011**, *32 (12)*, 2564-2574.

17. T. Clark, M. Hennemann, J. S. Murray, P. Politzer, *J. Mol. Mod.* **2007**, *13*, 291-296.

18. K. Eskandari, H. Zariny, *Chem. Phys. Lett.* **2010**, *491*, 9-13.

19. R. F. W. Bader, Atoms in Molecules: A Quantum Theory; Oxford University Press: Oxford, U.K., **1990.**

20. A. Forni, *J. Phys. Chem. A* **2009**, *113 (14)*, 3403-3412.

21. V. Tognetti, L. Joubert *Theor. Chem. Acc.* **2015**, *134*, 90.

22. W. Changwei, D. Danovich, Y. Mo, S. J. Shaik, *Chem. Theory Comput.* **2014**, *10*, 3726–3737.

23. S. F. Boys, *Rev. Mod. Phys.* **1960**, *32*, 296–299.

24. J. M. Foster, S. F. Boys, *Rev. Mod. Phys.* **1960**, *32*, 300–302.

25. C. Edmiston, K. Ruedenberg, *Rev. Mod. Phys.* **1963**, *35*, 457–465.

26. C. Edmiston, K. J. Ruedenberg, *Chem. Phys.* **1965**, *43*, S97–S116.

27. J. Pipek, P. G. J. Mezey, *Chem. Phys.* **1989**, *90*, 4916–4926.

28. R. McWeeny, *Proc. R. Soc. London Ser. A* **1959**, *253*, 242–259.

29. R. McWeeny, *Rev. Mod. Phys.* **1960**, *32*, 335–369.

30. R. McWeeny, In Methods of Molecular Quantum Mechanics, 2nd ed.; Academic Press: London, **1992**. Chapter 14, pp 485-495.

31. W. H. Adams, *J. Chem. Phys.* **1961**, *34*, 89-102.

32. S. Huzinaga, A. A. Cantu, *J. Chem. Phys.* **1971** *55*, 5543–5549.

33. T. L. Gilbert, *J. Chem. Phys.* **1974**, 60, 3835-3844.

34. O. Matsuoka, *J. Chem. Phys.* **1977**, *66*, 1245-1254.

35. H. Stoll, G. Wagenblast, H. Preuss, *Theor. Chim. Acta* **1980**, *57*, 169–178.

36. G. F. Smits, C. Altona, *Theor. Chim. Acta* **1985**, *67*, 461–475.

37. *E. Francisco, A. Martín Pendás, W. H. Adams, J. Chem. Phys.* **1992***, 97,* 6504-6508.

38. P. Ordejón, D. Drabold, M. Grumbach, R. Martin, *R. Phys. Rev. B* **1993***, 48,* 14646–14649.

39. M. M. Couty, A. A. Bayse, M. B. Hall, *Theor. Chem. Acc.* **1997***, 97,* 96–109.

40. A. Fornili, M. Sironi, M. Raimondi*, J. Mol. Struct. (THEOCHEM)* **2003***, 632,* 157–172.

41. Z. Szekeres, P. R. Surján, *Chem. Phys. Lett.* **2003**, *369*, 125–130.

42. M. Sironi, A. Genoni, M. Civera, S. Pieraccini, M. Ghitti, *Theor. Chem. Acc.* **2007**, *117*, 685-698.

43. A. Genoni, *J. Phys. Chem. Lett.* **2013**, *4*, 1093-1099.

44. A. Genoni, *J. Chem. Theory Comput.* **2013**, *9*, 3004-3019.

45. L. H. R. Dos Santos, A. Genoni, P. Macchi, *Acta Crystallogr., Sect. A* **2014**, *70*, 532-551.

46. A. Genoni, B. Meyer, *Adv. Quantum Chem.* **2016**, *73*, 333-362.

47. A. Fornili, M. Sironi, M. Raimondi, *J. Mol. Struct. (THEOCHEM)* **2003**, *632*, 157–172.

48. M. Sironi, A. Genoni, M. Civera, S. Pieraccini, M. Ghitti, *Theor. Chem. Acc.* **2007**, *117*, 685-698.

49. M. Sironi, A. Famulari, M. Raimondi, S. Chiesa, *J. Mol. Struct. (THEOCHEM)* **2000**, *529*, 47-54.

50. M. Sironi, M. Ghitti, A. Genoni, G. Saladino, S. Pieraccini, *J. Mol. Struct. (THEOCHEM)* **2009**, *898*, 8-16.

51. B. Meyer, B. Guillot, M. F. Ruiz-Lopez, A. Genoni, *J. Chem. Theory Comput.* **2016**, *12*, 1052-1067.

52. B. Meyer, B. Guillot, M. F. Ruiz-Lopez, A. Genoni, *J. Chem. Theory Comput.* **2016**, *12*, 1068-1081.

53. B. Meyer, A. Genoni, *J. Phys. Chem. A* **2018**, *122*, 8965-8981.

54. A. Genoni, M. Sironi, *Theor. Chem. Acc.* **2004**, *112*, 254-262.

55. A. Genoni, A. Fornili, M. Sironi, *J. Comput. Chem.* **2005**, *26*, 827-835.

56. A. Genoni, *Acta Crystallogr., Sect. A* **2017**, *73*, 312-316.

57. N. Casati, A. Genoni, B. Meyer, A. Krawczuk, P. Macchi, *Acta Crystallogr., Sect. B* 2017, *73*, 584-597.

58. L. J. McAllister, D. W. Bruce, P. B. Karadakov, *J. Phys. Chem. A* **2012**, *116*, 10621-10628.

59. J. Gerratt, W. N. Lipscomb, *Proc. Natl. Acad. Sci. U.S.A.* **1968**, *59*, 332-335.

60. P. B. Karadakov, J. Gerratt, D. L. Cooper, M. Raimondi, *J. Chem Phys.* **1992**, *97*, 7637-7655.

61. D. L. Cooper, J. Gerratt, M. Raimondi, M. Sironi, T. Thorsteinsson, *Theoret. Chim. Acta* **1993**, *85*, 261-270.

62. D. Jayatilaka, *Phys. Rev. Lett.* **1998**, *80*, 798-801.

63. D. Jayatilaka, D. J. Grimwood, *Acta Cryst. A* **2001**, *57*, 76-86.

64. A. Genoni, L. Bučinský, N. Claiser, J. Contreras-García, B. Dittrich, P. M. Dominiak, E. Espinosa, C. Gatti, P. Giannozzi, J.-M. Gillet, D. Jayatilaka, P. Macchi, A. Ø. Madsen, L. J. Massa, C. F. Matta, K. M. Merz Jr., P. N. H. Nakashima, H. Ott, U. Ryde, K. Schwarz, M. Sierka, S. Grabowsky, *Chem. Eur. J.* **2018**, *24*, 10881-10905.

65. S. Grabowsky, A. Genoni, H.-B. Bürgi, *Chem. Sci.* **2017**, *8*, 4159-4176.

66. A. Genoni, D. Franchini, S. Pieraccini, M. Sironi, *Chem. Eur. J.* **2018**, *24*, 15507-15511.

67. A. Genoni, L. H. R. Dos Santos, B. Meyer, P. Macchi, *IUCrJ* **2017**, *4*, 136-146.

68. In most of the situations it is sufficient to consider S=M. In the spin-coupled calculations for the present investigation we have always considered S=M=0.

69. B. H. Chirgwin, C. A. Coulson, *VI. Proc. R. Soc. London, Ser. A* **1950**, *201*, 196-209.

70. R. Ditchfield, W. J. Hehre, and J. A. Pople,, *J. Chem. Phys.* **1971**, *54*, 724-728.

71. G. Rumer, *Göttinger Nachr.* **1932**, *3*, 337-341.

72. M. Simonetta, E. Gianinetti, I. Vandoni, *J. Chem. Phys.* **1968**, *48*, 1579-1594.

73. M. J. Frisch, G. W. Trucks, H. B. Schlegel, G. E. Scuseria, M. A. Robb, J. R. Cheeseman, G. Scalmani, V. Barone, B. Mennucci, G. A. Petersson, H. Nakatsuji, M. Caricato, X. Li, H. P. Hratchian, A. F. Izmaylov, J. Bloino, G. Zheng, J. L. Sonnenberg, M. Hada, M. Ehara, K. Toyota, R. Fukuda, J. Hasegawa, M. Ishida, T. Nakajima, Y. Honda, O. Kitao, H. Nakai, T. Vreven, J. A. Montgomery, Jr., J. E. Peralta, F. Ogliaro, M. Bearpark, J. J. Heyd, E. Brothers, K. N. Kudin, V. N. Staroverov, R. Kobayashi, J. Normand, K. Raghavachari, A. Rendell, J. C. Burant, S. S. Iyengar, J. Tomasi, M. Cossi, N. Rega, J. M. Millam, M. Klene, J. E. Knox, J. B. Cross, V. Bakken, C. Adamo, J. Jaramillo, R. Gomperts, R. E. Stratmann, O. Yazyev, A. J. Austin, R. Cammi, C. Pomelli, J. W. Ochterski, R. L. Martin, K. Morokuma, V. G. Zakrzewski, G. A. Voth, P. Salvador, J. J. Dannenberg, S. Dapprich, A. D. Daniels, Ö. Farkas, J. B. Foresman, J. V. Ortiz, J. Cioslowski, and D. J. Fox, Gaussian 09 (Gaussian, Inc., Wallingford CT, **2009**).

74. D. L. Cooper, J. Gerratt, M. Raimondi, M. Sironi, T. Thorsteinsson, *Theoret. Chim. Acta* **1993**, *85*, 261.

GRAPHICAL ABSTRACT

Davide Franchini, Alessandro Genoni, Federico Dapiaggi, Stefano Pieraccini, and Maurizio Sironi

A valence bond description of the bromine halogen bond

Halogen bond is an interesting type of non-covalent interaction that is drawing lot of attention due to its possible application in several fields. In this paper, the nature of this interaction has been investigated using a Valence Bond approach. This enabled not only to confirm the main features of the previously proposed models (e.g., Politzer model), but also to shed further light on the physics of halogen bond, by introducing the new concept of σ-tunnel.

Politzer Model   **SC Method**